

FURTHER IMPROVED EDGE-DIRECTED INTERPOLATION AND FAST EDI FOR SDTV TO HDTV CONVERSION

Chi-Shing Wong and Wan-Chi Siu

Department of Electronic and Information Engineering, The Hong Kong Polytechnic University

ABSTRACT

High quality video interpolation is always desirable, since the definition of video display devices is improving. It is always necessary to port a video of lower quality to higher quality displays, such as the conversion of SDTV videos to HDTV videos. In this paper we will present a further improved Edge-Directed Interpolation (EDI) by proposing a new sampling pattern and subsequently give a fast approach for the enlargement of a SDTV (704×480) video into a HDTV (1280×720) video (1.5 time enlargement). Experimental results show that our approach has a better performance in terms of edge quality compared to that of the New Edge-Directed Interpolation (NEDI) in the literature. Moreover, the fast approach is 50% faster and the visual quality is also better than the NEDI.

1. INTRODUCTION

Image interpolation aims at reconstructing an image from a low-resolution to high resolution. It is well known that for classical linear interpolation approaches, such as bilinear and bicubic interpolation, they often suffer from edge blurring effect or produce an image with artifacts around the edge area [1]. Therefore, many research studies [2]-[9] tried to improve the visual quality of the increased resolution image by sharpening the edges and lowering the mean-squared errors and to make comparison with the linear interpolation techniques.

The quality of an interpolated image using traditional Edge-Directed interpolation methods [2]-[5] depends on the step for the detection of edge direction. As the traditional edge direction detection only quantizes edge orientations into a finite number of choices such as horizontal, vertical or diagonal directions, etc., this adversely affects the traditional Edge-Directed interpolation methods and limits the quality of the interpolated image. Hence, various types of the Edge-Directed interpolation methods have been further developed based on various statistical techniques, such as the covariance-based schemes [6]-[9]. The New Edge-Directed Interpolation (NEDI) [10] method is a typical example which possibly can give outstanding results.

A new direction on improving the visual quality of the New Edge-Directed Interpolation (NEDI) [10] can be done by changing step two of the interpolation in NEDI. The Improved New Edge-directed interpolation (IEDI) [11] was proposed in 2003. Subsequently, there have been some further improvements either on its objective or subjective quality, such as the Modified Edge Directed Interpolation (MEDI) [12]. The original NEDI involves two steps: (i) to

interpolate points with four symmetrical neighbours hence obtain the predicted value of the center unknown pixel, and (ii) to interpolate the rest of the points between the horizontal and vertical original pixels. The Modified algorithm MEDI has the same interpolation structure with the Improved algorithm IEDI [11] which modifies step two of the fourth order NEDI interpolation structure into a sixth order structure. It makes fuller use of the local relative information in low-resolution to get a high-resolution image with visually better quality. However, four out of six the data points that are used in the sixth order linear prediction equation in the MEDI are too far away from the unknown pixel, so it will introduce more prediction errors into the interpolated image.

In this paper, a Further Improved Edge-Directed Interpolation (FEDI) algorithm is proposed for image video interpolation, and we also propose a faster edge-directed interpolation to perform interpolation with an enlargement factor of 1.5 (Fast EDI-1.5). This new algorithm makes use of six nearest original image pixels and two predicted pixels to interpolate the unknown pixel. It can enhance the edge and reduce the prediction errors compared to that of the MEDI [12] interpolation structure. The fast interpolation approach makes a new interpolation step based on the edge-directed interpolation algorithm and eliminates unnecessary pixels to directly generate an image with 1.5 times, with lower computational cost. Although many papers have proposed new sampling patterns for the image interpolation, our approach aims at the conversion of SDTV to HDTV and has the lowest computational complexity. In this paper, we also give results of our study to minimize the number of the sample points using proposed algorithm and its effect on regions with high frequency.

2. THE PROPOSED ALGORITHM

2.1 FEDI

The Further Improved Edge-Directed interpolation (FEDI) makes use of the nearest original pixels and predicted pixels to form a new sampling pattern structure of the FEDI step two. This new structure can remove most of the worst estimated points in the MEDI and sharpen the edge of the image by making a full use of the local relative information in the low-resolution image.

The interpolation step one of the FEDI is the same as the NEDI, which makes uses of the fourth-order linear prediction to interpolate the unknown pixels $Y_{2i+1,2j+1}$ etc. (see Fig. 1).

In step two of the FEDI, we propose to use two interpolated results obtained from the NEDI first step to obtain the

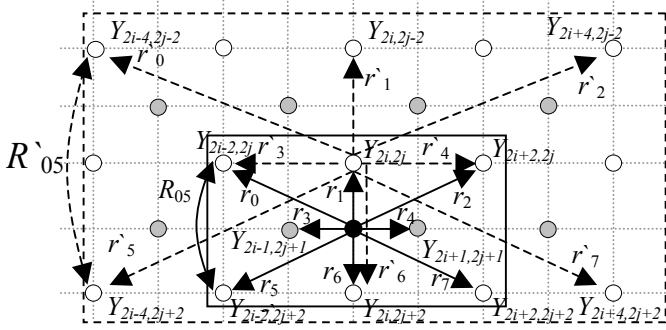


Figure 1. Illustrative example of FEDI step two

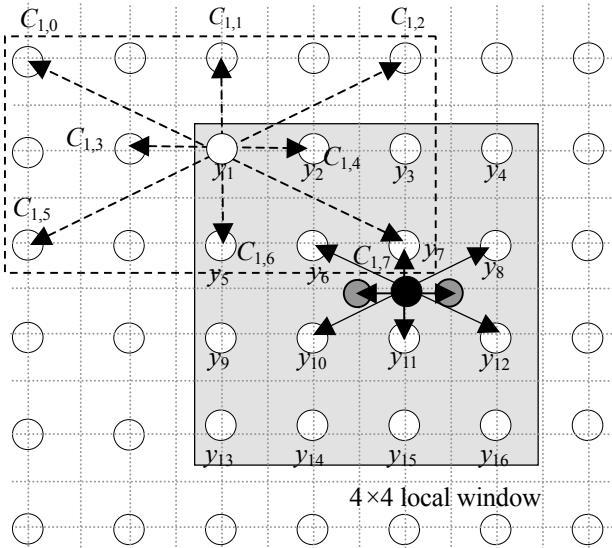


Figure 2. An example to illustrate the way of finding vector \mathbf{y} and matrix \mathbf{C} in step two of the FEDI

interpolation pixel which is indicated in black as shown in Figs. 1 and 2. Hence we interpolate the unknown pixel $Y_{2i,2j+1}$ (the black dots) by an eighth-order linear predictor from eight neighboring pixels given by the following equation:

$$Y_{2i,2j+1} = \sum_{l=0}^2 \alpha_l Y_{2(i+l-1),2j} + \sum_{l=0}^1 \alpha_{3+l} Y_{2(i+l)-1,2j+1} + \sum_{l=0}^2 \alpha_{5+l} Y_{2(i+l-1),2j+2} \quad (1)$$

where α_l are the coefficients of the linear predictor.

The white dots in Figs. 1 and 2 denote the original low-resolution pixels i.e. $X_{i,j}=Y_{2i,2j}$ and the gray dots denote the interpolation result from the NEDI step one. Moreover, in Figs. 1 and 3, the symbols r_l and r'_l represent the cross-covariance value in high-resolution and low-resolution, and symbols R_{kl} and R'_{kl} represent the auto-covariance value in high-resolution and low-resolution, respectively; also l and k mean the positions of the covariances.

According to Wiener filtering theory, the optimal Minimum Means Square Error (MMSE) prediction coefficients set $\boldsymbol{\alpha} = [\alpha_0, \alpha_1, \dots, \alpha_7]$, can be obtain as

$$\boldsymbol{\alpha} = \mathbf{R}_{yy}^{-1} \mathbf{r}_y \quad (2)$$

where the auto-covariance matrix \mathbf{R}_{yy} contains sixty-four R_{kl} , for $k, l = [0, \dots, 7]$, and the cross-covariance of \mathbf{r}_y contains eight r_l , for $l = [0, \dots, 7]$. The rest of the 2nd step interpolation points can also be obtained by a similar procedure, such as $Y_{2i+1,2j}$ can be computed by (3) below.

$$Y_{2i+1,2j} = \sum_{l=0}^2 \alpha_l Y_{2i,2(j+l-1)} + \sum_{l=0}^1 \alpha_{3+l} Y_{2i+1,2(j+l)-1} + \sum_{l=0}^2 \alpha_{5+l} Y_{2i+2,2(j+l-1)} \quad (3)$$

The high-resolution cross-covariance \mathbf{r}_y is not available now, because of the center pixel $Y_{2i,2j+1}$ is to be predicted. This difficulty can be overcome by the fact that the statistics of the pixels with respect to the low-resolution block and that of the high-resolution block are most likely to be similar. As a result, the auto-covariance and cross-covariance coefficients among the high-resolution block will be mostly alike that of the low-resolution block. Therefore, the low-resolution covariance \mathbf{R}'_{yy} and \mathbf{r}'_y will be used instead, for the calculation.

According to the classical covariance method, \mathbf{R}'_{yy} and \mathbf{r}'_y can be calculated by the following equation:

$$\mathbf{R}' = \frac{1}{M^2} \mathbf{C}^T \mathbf{C}, \quad \mathbf{r}' = \frac{1}{M^2} \mathbf{C}^T \mathbf{y} \quad (4)$$

where $\mathbf{y} = [y_1, \dots, y_{M \times M}]^T$ is a data vector containing $M \times M$ pixels inside a local window and \mathbf{C} is a $M^2 \times 8$ matrix,

$$\mathbf{C} = \begin{bmatrix} C_{1,0} & C_{1,1} & \dots & C_{1,6} & C_{1,7} \\ \dots & \dots & \dots & \dots & \dots \\ C_{k,0} & C_{k,1} & \dots & C_{k,6} & C_{k,7} \\ \dots & \dots & \dots & \dots & \dots \\ C_{M \times M,0} & C_{M \times M,1} & \dots & C_{M \times M,6} & C_{M \times M,7} \end{bmatrix}$$

whose k^{th} row vector contains its eight nearest neighbors of y_k as shown in Fig. 1. i.e. if $y_k = Y_{2i,2j}$, then the eight nearest neighbors are $\{Y_{2i-4,2j-2}, Y_{2i,2j-2}, Y_{2i+4,2j-2}, Y_{2i-2,2j}, Y_{2i+2,2j}, Y_{2i-4,2j+2}, Y_{2i,2j+2}, Y_{2i+4,2j+2}\}$ as shown in Fig. 1. In Fig. 2, if $y_k = y_1$, the eight nearest neighbors are $\{C_{1,0}, C_{1,1}, C_{1,2}, C_{1,3}, C_{1,4}, C_{1,5}, C_{1,6}, C_{1,7}\}$. When the local window is 4x4, vector \mathbf{y} and matrix \mathbf{C} can be find according to the structure as shown in the Fig. 2.

According to (2) and (4), we have

$$\boldsymbol{\alpha} = (\mathbf{C}^T \mathbf{C})^{-1} (\mathbf{C}^T \mathbf{y}) \quad (5)$$

After substituting $\boldsymbol{\alpha}$ into (1) and (3), we can compute the predicted values of $Y_{2i,2j+1}$ and $Y_{2i+1,2j}$, respectively.

2.2 Fast DEI with 1.5 times interpolation (Fast EDI-1.5)

In many practical applications, we always encounter the situation of converting a video from its original size to 1.5 of its size. For example, for converting a SDTV video to a HDTV video, we need a conversion ratio of 1.5 times. Let us try this conversion by proposing a new fast approach based on the edge-directed interpolation method in a block-based model.

The Fast EDI block-based model is shown in Fig. 3. The red box indicates the block size of each of the interpolation. In each interpolation, we consider eight unknown pixels (the black dots) inside the red box as shown in Fig. 3.

This Faster Edge-Directed Interpolation of 1.5 times (Fast EDI-1.5) only needs one-step to achieve the interpolation. We propose to make use of a fourth-order linear prediction to estimate eight unknown pixels at the same time by making use of (6)-(9) in this block-based model:

$$\text{For } c = 0, 2, 3 : Y_c = \sum_{k=0}^1 \sum_{l=0}^1 \alpha_{c,2k+l} X_{(i+k),(j+l)} \quad (6)$$

$$\text{For } c = 1, 4 : Y_c = \sum_{k=0}^1 \sum_{l=0}^1 \alpha_{c,2k+l} X_{(i+k+1),(j+l)} \quad (7)$$

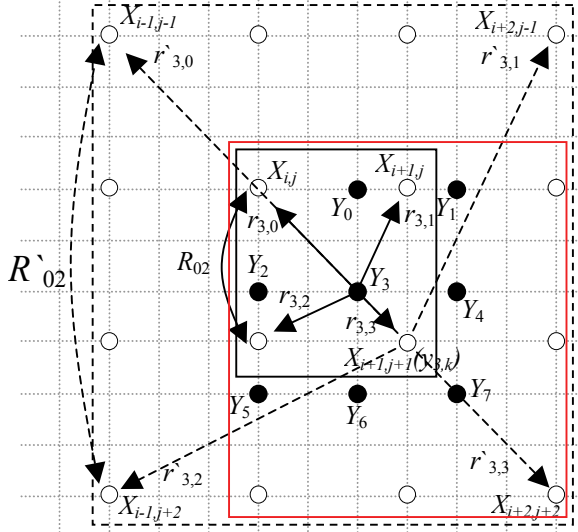


Figure 3. Illustrative example of interpolation step in Fast EDI-1.5 using block-based model

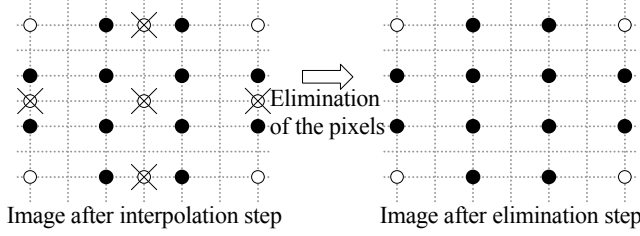


Figure 4. Illustrative example of elimination step in Fast EDI-1.5

$$\text{For } c = 5, 6 : Y_c = \sum_{k=0}^1 \sum_{l=0}^1 \alpha_{c,2k+l} X_{(i+k),(j+l+1)} \quad (8)$$

$$\text{For } c = 7 : Y_c = \sum_{k=0}^1 \sum_{l=0}^1 \alpha_{c,2k+l} X_{(i+k+1),(j+l+1)} \quad (9)$$

Coefficients $\alpha_c = [\alpha_{c,0}, \alpha_{c,1} \dots \alpha_{c,3}]$ can be calculated from (2) with the auto-covariance \mathbf{R}_{yy} matrix containing sixteen R_{kl} with $k, l = [0, \dots, 3]$ and for $c = [0, \dots, 7]$. There are totally eight cross-covariances, $\mathbf{r}_{0,y}, \mathbf{r}_{1,y}, \dots, \mathbf{r}_{7,y}(\mathbf{r}_{c,y})$. Each of them contains four $r_{c,l}$ with $l = [0, \dots, 3]$. As the high-resolution covariance $\mathbf{r}_{c,y}$ is not available, the low-resolution covariance \mathbf{R}_{yy} and $\mathbf{r}_{c,y}$ are used for the computation. Fig. 3 shows some details of estimating pixel Y_3 . The white dots in Fig. 3 are original pixels and black dots are pixels to be interpolated.

Again \mathbf{R}_{yy} and $\mathbf{r}_{c,y}$ can be calculated by:

$$\mathbf{R} = \frac{1}{M^2} \mathbf{C}^T \mathbf{C}, \quad \mathbf{r}_c = \frac{1}{M^2} \mathbf{C}^T \mathbf{y}_c \quad (10)$$

where $\mathbf{y}_c = [y_{c,1} \dots y_{c,k} \dots y_{c,M \times M}]^T$ is the data vector containing the $M \times M$ pixels inside a local window for a special position c and \mathbf{C} is a $M^2 \times 4$ data matrix whose k^{th} row vector contains the four nearest neighbors of $y_{c,k}$, i.e. if $y_{3,k} = X_{i+1,j+1}$, then the four nearest neighbors are $\{X_{i-1,j-1}, X_{i+2,j-1}, X_{i-1,j+2}, X_{i+2,j+2}\}$.

The difference between equus. (10) and (4) is that equ. (10) making use of the eight cross-covariance function $\mathbf{r}_0, \mathbf{r}_1, \dots, \mathbf{r}_7$ at the same time with only one auto-covariance function \mathbf{R} inside the red box as shown in Fig. 3. It can be done because we estimate the eight unknown pixels (Y_0, Y_1, \dots, Y_7) at the same time by using four known pixels $\{X_{i-1,j-1}, X_{i+2,j-1}, X_{i-1,j+2}, X_{i+2,j+2}\}$ in this block-based model.

From (5), we can find the filter coefficients, α_c , and then the interpolated value of the Y_c can be obtained by substituting α_c into (6)-(9) according to the position of c .

Finally, after the eight pixels $Y_0, Y_1 \dots Y_7$ have been estimated, three original pixels $X_{i+1,j}, X_{i,j+1}$ and $X_{i+1,j+1}$ need to be deleted, so that the image is scaled up properly by 1.5 times. This is the elimination step which is shown in Fig. 4.

3. EXPERIMENTAL RESULTS

A set of the color images is used for comparing the performance in terms of PSNR among NEDI, MEDI and FEDI, with two images as shown in Figs. 5 and 6. We extract intermediate results of some steps in order to illustrate the effect of various approaches. All the programs were written in C++ language and run on the same platform.

The test images with size $2H \times 2W$ were firstly down-sampled by a factor of 2 to images of size $H \times W$. The down-sampled images were then enlarged with a factor of 2 to $2H \times 2W$ using the NEDI, MEDI and FEDI.

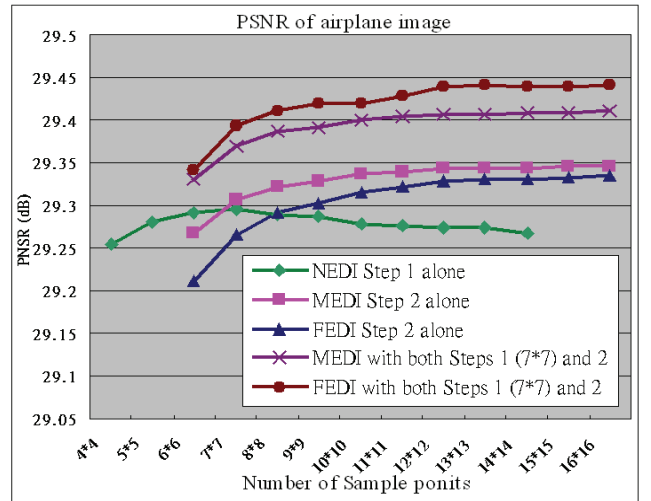


Figure 5. PSNR of airplane image by FEDI and MEDI

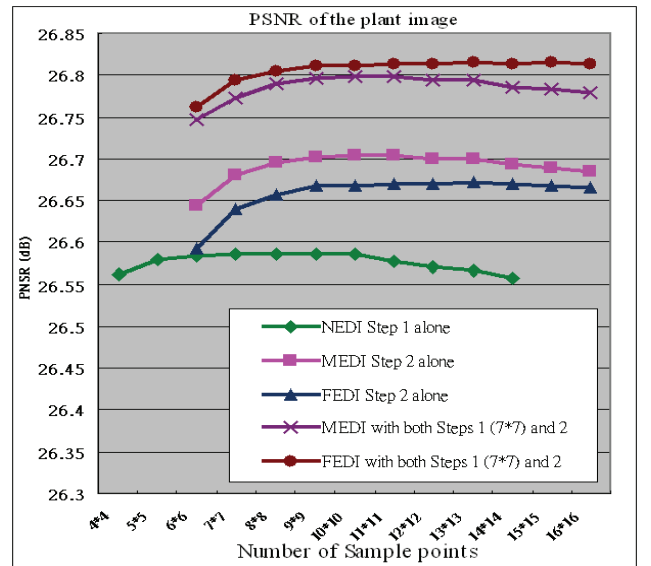


Figure 6. PSNR of plant image by FEDI and MEDI

For each of the figures, there are five PSNR curves. For the curve with “NEDI Step 1 alone” (green), it is the PSNR of the image after performing the NEDI Step 1 with different numbers of the sample points. Both “MEDI step 2 alone” (pink) and “FEDI Step 2 alone” (blue) curves are the PSNR values of the image after performing the interpolation step two only with different numbers of sample points. For the last two: “MEDI with both Steps 1 (7×7) and 2” (purple) and “FEDI with both Steps 1 (7×7) and 2” (red) curves, we interpolated both images by making use of the NEDI step 1 with sample points equal to 7×7 , and varied the number of sample points in interpolation step two from 6×6 to 16×16 .

In both figures, it is obvious that the PSNR of “FEDI step 2 alone” (blue) is much lower than that of the “MEDI step 2 alone” (pink), because the FEDI step two requires two predicted results from step one prediction. However, when we interpolated the image by MEDI and FEDI with both steps one and two, we can see that our FEDI results (red) in a higher PSNR than MEDI (purple) for using any number of sample points in interpolation step two. The comparison of the visual quality between FEDI and MEDI is shown in Fig. 7. We can see that our proposed FEDI can achieve a sharper image (see Fig. 7: b and d) with less artifacts (uneven pixels inside the red ellipses as shown in Fig. 7: a and c) than that of the MEDI.

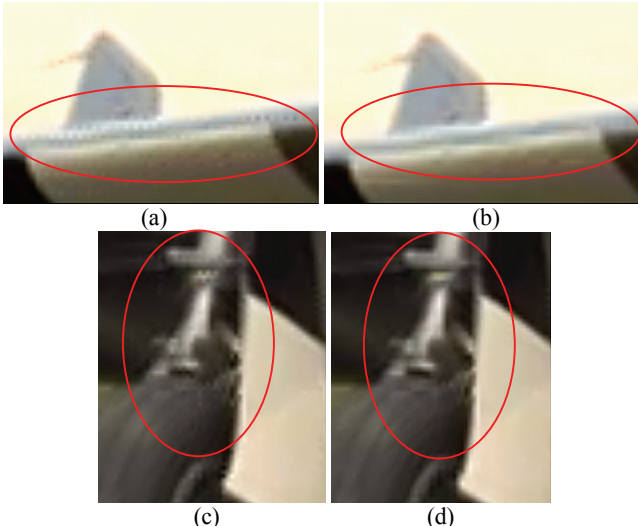


Figure 7. Portions of the airplane image: (a) and (c) reconstructed image by MEDI (PSNR=29.37 dB), (b) and (d) reconstructed image by FEDI (PSNR=29.39 dB).

In some rare cases, such as Fig. 8 the PSNR of FEDI is slightly lower than the PSNR of the NEDI, the visual quality of FEDI is still better than NEDI. In Fig. 8, we can see that using the FEDI for magnification, it results in a sharper image with more continuous edges than the NEDI.

Note from Figs. 5 and 6 that the PSNR values of the FEDI with both steps one and two increase initially and then decrease. It means that an increase in the number of sample points may not be able to improve the PSNR. Hence, there is an optimal number of the sample points for using the FEDI. According to the experiment results, we have found that the optimal number of the sample points in step one is between 6×6 and 8×8 and in step two is between 8×8 and 12×12 . This result can also apply to the MEDI schemes.



Figure 8. Portion of the lady image: (a) reconstructed image by NEDI (PSNR=30.15 dB), and (b) reconstructed image by FEDI (PSNR=30.11 dB).

Most of the interpolation schemes based on the edge-directed interpolation give a poor performance (unwanted colour and thick lines inside of the red ellipses in Fig. 9: a-d) on high frequency regions of an image. This is because when the image contains high frequency regions, the low-resolution covariance cannot estimate this high frequencies covariance structure accurately. However, we find that this mismatch problem can be resolved by increasing the number of sample points. We directly interpolated the lighthouse image by our FEDI from 512×768 to 1024×1536 with different numbers of sample points. Since we only want to compare the visual quality on the high frequency region, no downsampling is required and the PSNR is not the subject in this simulation. Some results are shown in Fig. 9. We can see that when the number of the sample points increased, the visual quality of the high frequency region is improving, by removing the undesirable prediction pixels as shown inside of the red ellipses in Fig. 9: e and f.

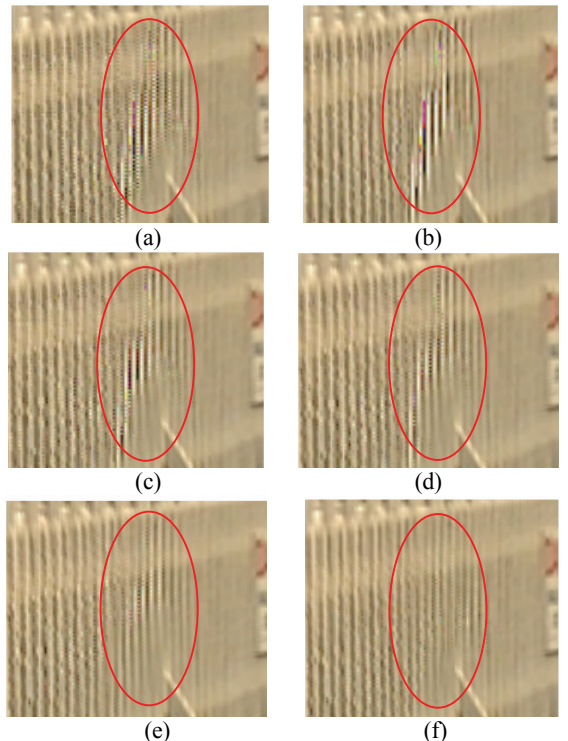


Figure 9. Portions of the lighthouse image, reconstructed by the FEDI with different numbers of sample points (a) using 7×7 , (b) using 8×8 , (c) using 9×9 , (d) using 11×11 , (e) using 13×13 and (f) using 16×16 .

For enlarging a SD video to a HD video, the visual quality of Fast EDI-1.5 is better than the NEDI results which were to scale up the image by 2 times and than to downsample the results by a factor $\frac{3}{4}$, so that it has the same interpolation factor. From Figs. 10 and 11, we can see that our proposed Fast EDI-1.5 can interpolate a sharpen image than the NEDI. It is because the Fast EDI-1.5 does not need an addition down-sampling operation. Hence it can preserve the sharpness of the image. That is, the NEDI needs an addition step of downsample operations to perform the 1.5 time enlargement, which accounts for the smoothing effect on the interpolated image. In additional, the computational cost of the Fast EDI-1.5 is about 50% of NEDI (see Table 1).

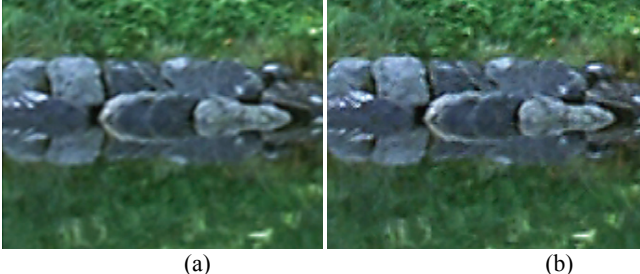


Figure 10. Portions of the interpolated Pak Joy image from SD to HD: (a) reconstructed by NEDI and then downsampling by a factor $\frac{3}{4}$, and (b) reconstructed by Fast EDI-1.5 (ours).

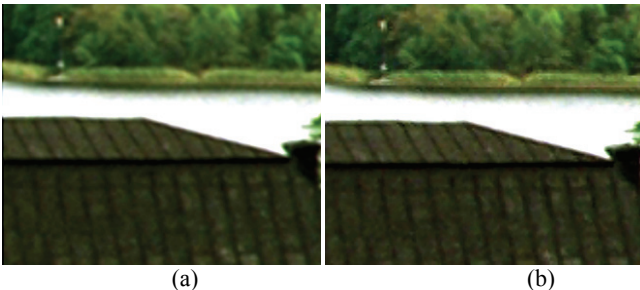


Figure 11. Portions of the interpolated InTo Tree image from SD to HD: (a) reconstructed by NEDI and then downsampling by a factor $\frac{3}{4}$, and (b) reconstructed by Fast EDI-1.5 (ours).

Table 1. Interpolation time of SD image to HD image

Name Of The Image	NEDI	Fast EDI-1.5	Time reduce of Fast EDI-1.5 Scheme Compared To NEDI
Ducks Take Off	14.5s	6.8s	-53%
Pak Joy	8.1s	3.7s	-54%
Crowd	12.2s	5.7s	-53%
InTo Tree	10.4s	5.4s	-48%
Old Town Cross	9.8s	4.9s	-49%

4. CONCLUSION

We have proposed the Further Improved Edge-directed Interpolation scheme (FEDI) and applied the EDI concept to scales up an image to 1.5 times (Fast EDI-1.5) in this paper. Both FEDI and Fast EDI-1.5 can be used in the interpolation of a SDTV video to a HDTV video. The proposed FEDI scheme has a better visual quality compared with that of the MEDI scheme, and has a sharper edge as compared to the NEDI scheme, but it requires a high computational cost. Hence, we have developed a fast scheme, Fast EDI-1.5, which has a better visual quality compared with the NEDI

and with less computational cost. We also have suggested a possible optimal number of sample points and given the effect on the number of sample points for high frequency regions. Much further work can be done on improving the Fast EDI-1.5 approach by making use of the FEDI scheme and making further improvement by using some multi-frame super-resolution techniques.

5. ACKNOWLEDGEMENT

This work is supported by the Centre for Signal Processing, the Hong Kong Polytechnic University and the Research Grant Council of the Hong Kong SAR Government (PolyU 5278/08E).

REFERENCES

- [1] J.A. Parker, R.V. Kenyon and D.E. Troxel, "Comparison of interpolating methods for image resampling", *IEEE Trans. on Medical Image*, vol.2, pp.31-9, Mar. 1983.
- [2] J. Allebach and P.W. Wong, "Edge-Directed Interpolation", *Proc. of IEEE Int. Conference on Image Processing (ICIP 1996)*, vol.2, pp.707-710, Sept. 1996, Switzerland.
- [3] S.D. Bayraker and R.M. Mersereau, "A new method for directional image interpolation", *Proc. of Int. Conference on Acoustics, Speech, and Signal Processing (ICASSP 1995)*, vol.4, pp.2383-6, May, 1995, Atlanta USA.
- [4] Q. Wang and R. Ward, "A new edge-directed image expansion scheme", *Proc. of IEEE Int. Conference on Image Processing (ICIP 2001)*, vol.1, pp.899-902, Oct. 2001, Thessaloniki Greece.
- [5] Y. Cha and S. Kim, "The error amended sharp edge (EASE) scheme for image zooming", *IEEE Trans. on Image Processing*, vol 16, no.6, pp1496-1505, Jun. 2007.
- [6] X. Li and M.T. Orchard, "Edge-Directed Prediction for lossless Compression of Natural Images", *IEEE Trans. on Image Processing*, vol.10, no.6, pp.813-7, Jun. 2001.
- [7] N. Asuni and A. Giachetti, "Accuracy Improvements and Artifacts removal in Edge Based Image Interpolation", *Proc. of International Conference on Computer Vision Theory and Applications (VISAPP 2008)*, pp. 58–65, 22-25 Jan. 2008, Funchal Madeira Portugal.
- [8] X. Zhang and X. Wu, "Image Interpolation by Adaptive 2-D Autoregressive Modeling and Soft-Decision Estimation", *IEEE Trans. on Image Processing*, vol. 17, no. 6, pp. 887–896, Oct. 2008.
- [9] D.D. Muresan and T.W. Parks, "Adaptively Quadratic (Aqua) Image Interpolation", *IEEE Trans. on Image Processing*, vol. 13, no. 5, pp.690-8, May 2004.
- [10] X. Li and M.T. Orchard, "New Edge-Directed Interpolation", *IEEE Trans. on Image Processing*, Vol.10 No.10, pp.1521-7, Oct. 2001.
- [11] X.Q. Chen, J. Zhang and L.N. Wu, "Improvement of a nonlinear image interpolation method based on heat diffusion equation", *Proc. of International Conference on Machine Learning and Cybernetics (ICMLC 2003)*, vol.5, pp.2911-4, 2-5 Nov. 2003, Xi-an China.
- [12] W.S. Tam, C.W. Kok and W.C. Siu, "A Modified Edge Directed Interpolation for Images", *Proc. 17th European Signal Processing Conference (EUSIPCO 2009)*, pp.283-7, 24-28 Aug. 2009, Glasgow U.K.